

3D Zonation model of primary haloes and geochemical prospecting pattern of Aliabad Cu-Mo deposit, Yazd, Central Iran

Mahdi Bemani¹, Seyyed Hossein Mojtahedzadeh^{*1}, Abdolhamid Ansari¹

1- Department of Mining and Metallurgical Engineering, Yazd University, Yazd, Iran

* Corresponding Author: hmojtahed@yazd.ac.ir
(Received: November 2019, Accepted: March 2020)

Keywords

Aliabad porphyry Cu-Mo deposit
primary halos
Geochemical zonality
Zonality index
Block model

Abstract

Most hydrothermal ore deposits are controlled by geological structures. They are often a product of multistage hydrothermal activities, as a result, primary alteration haloes usually overlap in the vertical direction. By distinguishing the hydrothermal stages associated with ore-forming processes, one can determine the timings of hydrothermal activities and use the results as a method to identify blind mineralization. In order to explore probable blind mineralized zones of the Aliabad deposit, it is necessary to evaluate the element concentrations towards the depth or margins of the deposit. Modeling primary geochemical haloes could be useful in this

stage. The Aliabad porphyry Cu-Mo deposit, located in the southern segment of Central Iran and adjacent to the northern border of the Urmia-Dokhtar volcanic belt and east of the Dehshir fault. Ore bodies at the Aliabad deposit are primarily controlled by structural features, which provide an opportunity to investigate the zonality in primary halos in this copper-molybdenum porphyry deposit. The primary geochemical characteristics of the mineral deposit were studied based on geochemical analysis of 1559 core samples from 24 drill holes. The formation of the primary geochemical haloes, which joins the ore body up to the surface, can be associated with hydrothermal fluid diffusion through fracture (fissures) zone developed in the rocks of the folding axis in the mining area. Along the vertical direction, the concentrations of Cu, Ag, and Fe shows an increasing trend from the surface to the ore body, at all boreholes; while the concentration of Pb, Mn, and Bi are decreased with depth at the same environment. A detailed zonality sequence of indicator elements is obtained using the variability index of these elements: $Pb \rightarrow (Bi, Mn, Mo) \rightarrow Cr \rightarrow Ni \rightarrow (Sb, V, Zn) \rightarrow (Ag, Co, Cu, Fe, S) \rightarrow P$. According to this zonality, indexes such as $Vz4 = Pb \times Mn / Cu \times Ag$ and $Vz5 = Pb \times Mn / Cu \times Ag \times Co$ can be constructed and considered as a significant criterion for predicting the Cu potential at a particular depth. Studying the distribution of the zoning indexes at different levels revealed high values of proposed indexes in the northwest and south of the area. It can be concluded that copper mineralization will continue to deeper and unexplored parts of the deposit northwest of the study area. Consequently, it is suggested that further investigations concentrate on geophysical operations and it is highly recommended to drill additional boreholes at these areas. It is noteworthy that new drillings of the northwestern part must continue deeper than current boreholes (>150 m); because geochemical zonality indexes are extended to deeper parts. This extension is not observed for the southern part, so, additional drillings at the southern part can be shallower than 150 m.

1- INTRODUCTION

The primary geochemical halo of a mineral deposit was originally defined by Safronov (1936) as 'an environment including enriched ore-forming and associated elements which is formed by hydrothermal ore processing'. Thus, research on primary haloes may form part [1] of a mineral deposit model, but both the deposit model and primary halo approaches are based on studies of primary geochemical features of mineral deposits [2]. These features are the essential mechanisms for metal precipitation or mineral formation and are indicative of chemical processes that occur during mineralization [3].

Primary haloes of mineral deposits are results of interactions between country rocks and mineralizing fluids and can be characterized by element/metal enrichment/depletion (e.g., [1,4-5]) and/or mineral alterations (e.g., [6-7]). Geochemical characteristics of primary haloes of the mineral deposits are quite predictable and explicable., there are many studies on prospecting the mineral deposits through primary geochemical characteristics, all of which suggested that hydrothermal primary haloes (or anomalies) exist around polymetallic mineral deposits and summarized the methods and techniques of prospecting the mineral deposits through primary haloes (e.g., [5,8-9]). Meanwhile, indicators used in litho-geochemical prospecting have been proposed. Documents concerning geochemical exploration and

research on copper and lead-zinc deposits of various types discussed a combination of elements associated with the mineral deposits and set up indicators in geochemical prospecting for such mineral deposits (e.g., [10-11]).

The primary geochemical characteristics from drilling exploration after the discovery of the mineral deposits were studied. In 2009, a primary geochemical halo survey was carried out using the surface and drill core samples for the Donggua Mountain mineral deposit based on the idea that a structural fissure zone occurring in the axial belt of the anticline could provide migration channels for ore-forming fluids in the process of copper mineralization [5,9].

Primary haloes are multi-component; therefore, it is necessary to compare haloes of different elements to choose the appropriate indicator elements [8,12]. Primary halos of mineral deposits at different depths are characterized by specific values of a geochemical zonality (Vz) index the practical exploration significance of a Vz index is for recognition of erosional surfaces representing vertical levels of geochemical anomalies [13].

Primary geochemical halo survey is an effective method for prospecting the mineral deposits. However, the investigations on primary geochemical characteristics of concealed mineral deposits are very limited. Therefore, this paper, with the Aliabad copper-molybdenum deposit located in central Iran as an example, attempts to discuss the primary geochemical patterns for such concealed mineral deposits and erosional surfaces of geochemical anomalies.

2- REGIONAL GEOLOGY AND MINERALIZATION

Aliabad copper deposit is located at Khezrabad geological map which is a part of the southern section of the Central Iran geological district (Fig. 1. a). This area is adjacent to the northern borders of the Urmie-Dokhtar magmatic belt and the Dehshir fault [14]. Regarding the geological settings and the age of intrusive and surrounding rocks, the Aliabad area cannot count as a part of the Uremia-Dokhtar magmatic belt. On the other hand, most of the porphyry copper deposits of Iran are located at this belt, and in some references, the Aliabad area is considered as a part of the Uremia-Dokhtar magmatic belt [15].

Regarding Khezrabad geological map, the area is mostly covered by Granitic rocks, quaternary sediments, and also dacite rocks. Jurassic Granites are the oldest rock unit in the Aliabad area and they are non-continuously covered by volcano-sediment units with the age of Cretaceous [16]. Sangestan formation which is commonly made of clastic rocks (shale and sandstone) forms a discontinuity with the Shirkuh granite at the lower part.

Upperparts of the Sangestan formation are covered by a dolomitic limestone unit which is a part of Taft formation. Based on fossil studies, this unit belongs to the Cretaceous age. Taft formation starts with shaly limestone to thin-bedded limestone and at the upper parts, it changes into thick-bedded limestone, which forms high grounds. The geological and alteration map of the study area has prepared based on in-detail field surveys at a 1:1000 scale (Fig. 1. b). Geological units of the Aliabad area can be divided into 5 parts including granite (gr), Cretaceous volcano-sediments (K^c , K^{ct} , K^t , K^d and K^{qz}), dykes and silicic veins (g^{dp} and Si), brecciated and fractured areas, and quaternary deposits (Q^s , Q^{al} , Q^l).

the Urmia-Dokhtar volcanic belt, which is extended from NW to SE Iran, has a wide variety of metallic deposits and the Aliabad deposit is located among the northern border of this belt and the southern segment of Central Iran and east of the Dehshir fault (Fig. 1. a). The geological map and alteration of the study area are shown in Fig. 1.b. The copper mineralization occurrence is restricted to Malachite and Azurite veinlets, rarely Pyrite and Chalcopyrite, and scarcely chalcocite and covellite grains. The mineralization displays stockwork textures and is disseminated in the altered host rocks.

3- ALTERATION

The extent and intensity of alterations depend on the volume of magmatic solutions, the primary and secondary fractures, and the chemical composition of the host rocks. Also, deep faults have created suitable passages for easier movement of hydrothermal solutions and facilitate their rotation, and consequently, increased the alteration intensity. In an ideal porphyry copper deposit model, a core made of quartz and potassium-bearing minerals (mostly potassium feldspar and biotite) is surrounded by multiple hydrous zones of alteration minerals (Fig. 2) [17-18].

The study area has been severely affected by the alteration. The processing of satellite data in various methods shows the vast alteration in the region [19]. The extent of alteration is directly related to the extension of intrusive masses. Expected alterations in porphyry copper mineralizations are present in the study area, however, based on field surveys, X-ray studies, and petrography of rock and mineral samples, Potassic alteration does not exist at the surface [19]. Phyllic alteration comprises a large part of the study area. Almost all granite outcrops at the central part of the area are affected by this alteration.

The formation of new clay minerals in silicate rocks indicates argillic alteration [20]. In the Aliabad deposit, argillic alteration is found in small and scattered areas within the phyllic alteration zone. In the northeast of the area, the tuff unit has been locally affected by argillic alteration. In addition to the aforementioned areas, there are other argillic

alteration sites, which are identified on the geological map (Fig. 1. b)

Propylitic alteration is characterized by the appearance of secondary calcium and magnesium minerals [21] and is sometimes assumed to be equivalent to greenschist facies metamorphism.

Propylitic alteration is commonly observed at the margins of porphyry deposits [22]. Propylitic alteration is observed in the study area in the northeast and southwest of the area and around the phyllic alteration zone. There are limited siliceous veins in the rocks in this area.

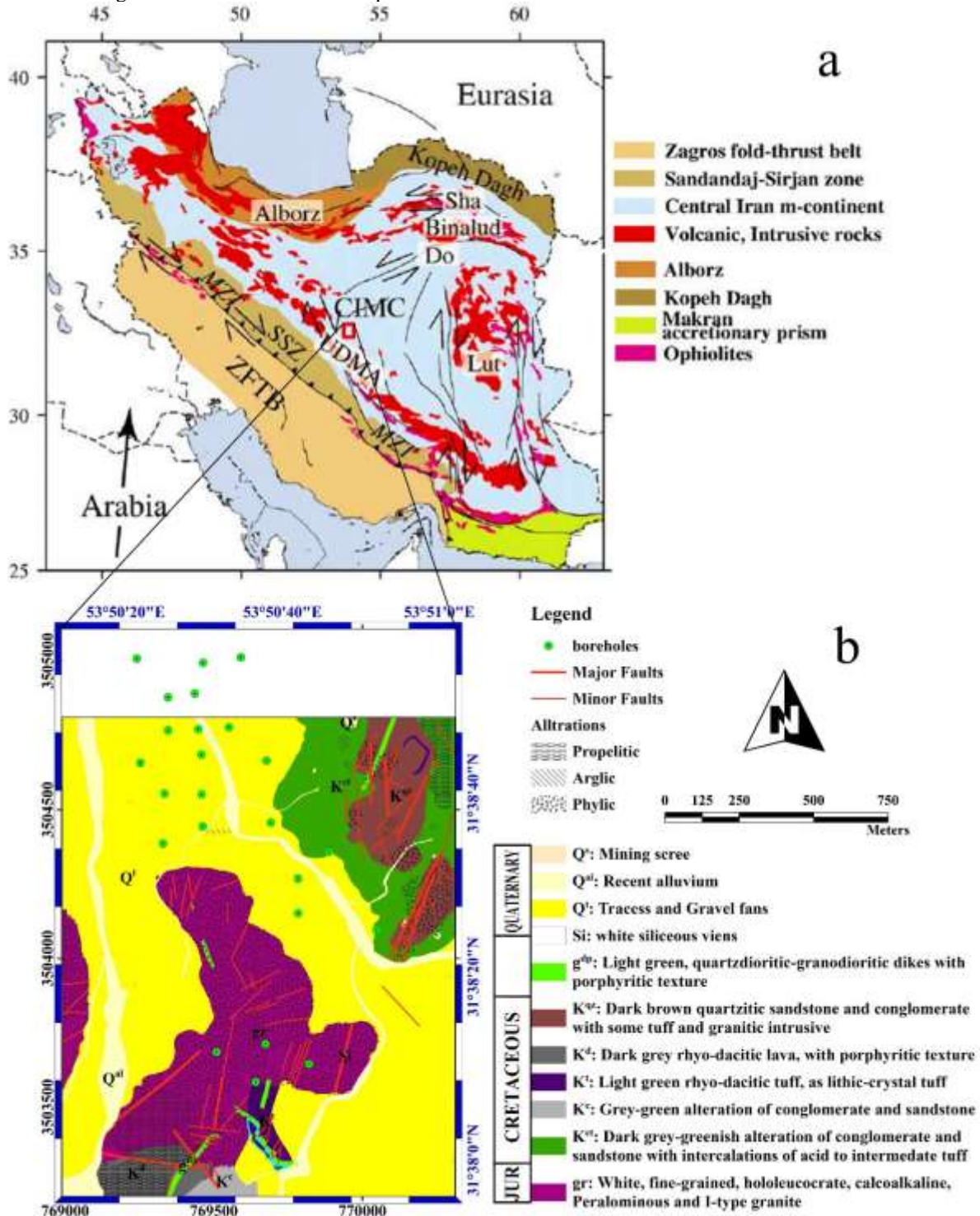


Fig. 1- a. Simplified geological map of Iran showing the main tectonic regions. ZFTB: Zagros fold-thrust belt; SSZ: Sanandaj-Sirjan zone; MZT: Main Zagros thrust; UDMA: Urumieh-Dokhtar magmatic assemblage; CMC: Central Iran micro-continent. Do is the Doruneh fault and Sha is the Shahrud fault[23]. b. geological map showing the alteration and geology units in the study area.

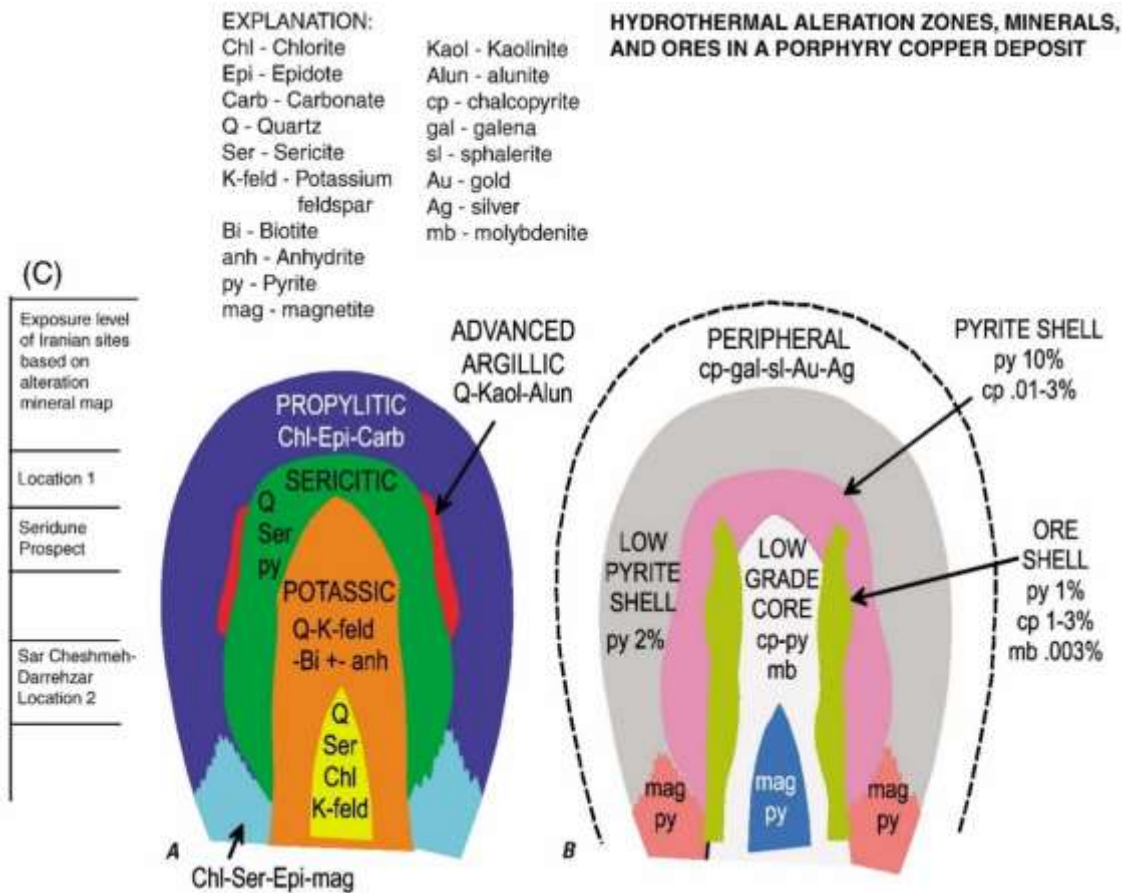


Fig. 2-. Illustrated deposit model of a porphyry copper deposit (modified from [19]). (A) Schematic cross-section of hydrothermal alteration minerals and types, which include propylitic, sericitic, advanced argillic, and potassic alteration. (B) Schematic cross-section of ores associated with each alteration type. (C) Scale showing level of interpreted exposure for Iranian alteration sites based on ASTER mapped alteration units [18]

4- MATERIALS AND METHODS

For an in-detail exploration of the Aliabad deposit, previous studies had been done in terms of detailed petrologic and geological studies. Moreover, detailed alteration and mineralogical studies have been carried out in the study area [19]. The deposit is explored via two-stage core drilling projects. At the first stage, 50 boreholes were drilled and core samples were analyzed for copper, molybdenum, and copper oxide concentrations. At the second stage, additionally, 24 boreholes were drilled to the maximum depth of 215 m and 1559 obtained samples were analyzed using the ICP-OES method. Reported concentrations of Ag, Bi, Co, Cr, Cu, Fe, Mn, Mo, Ni, P, Pb, S, Sb, V, Zn in ppm and percentages were considered as the main basis of the present study. Table 1 is showing the primary statistics of the used data. Outliers data are replaced

by the values obtained from the Cohen Maximum Likelihood method. In order to distinguish deep blind mineralization and the erosional surface of the deposit, zonality index methods were used. In practice, it is mandatory to create a 3D block model and estimate all concentrations in the whole domain. This is done by a geostatistical procedure of using ordinary log-kriging. Having all concentrations at the 3D domain, it is possible to calculate the surface production power for all elements at the desired level. A fractal-based Concentration-Volume (C-V fractal) method is used to obtain all possible thresholds for all elements at the domain. At the next step, the geochemical zonality index of all 15 elements was modeled using surface production power at all levels; and then, based on the acquired zonality index (Vz), blind mineralization potential at depth and also the erosional surface of the deposit can be determined.

Table 1-. Basic statistical parameters

Variable	Number of samples	Mean	StDev	Minimum	Maximum	Skewness	Kurtosis
Ag (ppm)	1559	1.40	3.04	1	41	6.43	63.49
Bi (ppm)	1559	0.35	3.86	1	80	13.14	197.19
Co (ppm)	1559	8.12	10.72	2	109	1.95	9.92
Cr (ppm)	1559	11.38	19.27	7	303	4.66	50.97
Cu (%)	1559	0.21	0.35	0.0006	5.57	7.53	86.16
Fe (%)	1559	3.18	2.43	0.25	40.4	5.08	54.22
Mn (%)	1559	0.03	0.07	0.0013	0.93	5.14	36.48
Mo (ppm)	1559	17.70	39.51	3.33	1110	15.43	386.24
Ni (ppm)	1559	18.59	31.75	3.7	540	8.25	110.87
P (ppm)	1559	481.66	239.76	33	2340	1.85	8.66
Pb (ppm)	1559	73.64	212.18	13.33	3320	7.56	75.32
S (%)	1559	2.15	1.78	0.007	13.03	1.4	3.2
Sb (ppm)	1559	0.18	3.00	0.35	85	20.53	486.17
V (ppm)	1559	18.39	19.47	3.33	137	1.63	3.57
Zn (ppm)	1559	257.90	511.70	4	8600	7.75	81.17

5- GEOSTATISTICS

In order to have a 3-D vision of grade changes along with the whole domain, one possible way is using geostatistical methods, based on core samples data. The result will be reported in the form of block models. A preprocessing stage is mandatory to achieve a reliable and accurate geostatistical model; especially when the data contains concentrations of trace or rare elements such as copper, molybdenum, etc.

In such cases, outlier detection/ replacement is critical. It is also the same for the shape of distributions, functions [24]. In this study, most of the measured concentrations show long tails distribution. Using geostatistical methods, such as ordinary kriging on the raw form of these data is valid but not optimum. Because estimation of values at the long tails will result in both smoothing valuable anomalies and a systematically increasing of estimation error. A simple but effective solution is to use simple log-transformed values instead of their raw Values. The combination of this transformation with kriging is called log- kriging. Studying the core sample data revealed that there is no significant censored data. Also, most of the core samples gathered from 2m core length. Therefore, it is decided to set the composite length as 2m. Raw and log-transformed Concentrations show no considerable trend among three coordinate axes. The next step is the variogram calculation and modeling. It can be seen in Fig. 3 that most of the elements show one structure-exponential variogram. Suitable models were fitted on experimental variograms at three axes of anisotropy ellipsoids. Table 2 shows

the anisotropy factors of the analyzed elements at the Aliabad deposit. Bi and Ni are showing weak anisotropy, while S and Cu are showing strong anisotropy. Fig. 3 only shows the modeled variograms along with the major axis of anisotropy.

The variogram of Molybdenum shows a small range of 30 m. This is due to the lack of samples in 3D space. Also, a limited variogram range of 100 m for the other elements is observed. This happens because boreholes are sparse.

Using variogram models, ordinary kriging was performed to estimate 15 elements over a 20*20*20 m block model. For example, Cu and Pb block models are illustrated in Fig. 6 and Fig. 7 respectively. High Copper bearing blocks are located northwest of the deposit.

6- C-V FRACTAL MODEL

Afzal et al. [25] have proposed C-V fractal models to delineate different levels of mineralization in different ore deposit types. On the C-V log-log plot, it can be observed that where the slope of the curve changes, which represents an intensive change in the geochemical population, which is in turn affected by changes in geological and mineralization characteristics. In general, modeling is defined using the following formula:

$$V(\rho \leq v) \propto \rho^{-a1}; \quad V(\rho > v) \propto \rho^{-a2} \quad (1)$$

where $V(\rho \leq v)$ and $V(\rho > v)$ indicate volumes (V : m³ in this study) with ore values (ρ : % or ppm in this study) which are smaller and greater than, respectively, the threshold values (v : % or ppm in this research) that define those volumes; $a1$ and $a2$ are characteristic exponents. In this model, threshold values represent boundaries between the various

types of mineralized zones (including barren host rocks) within the different mineral deposits. To calculate $V(\rho \leq v)$ and $V(\rho > v)$, in a 3D model representing the volumes enclosed by block model ρ , core sample data can be interpolated or simulated using geostatistical estimation/simulation methods [26-27].

Distinct patterns, corresponding to a set of similarly shaped block models, can be separated by different straight segments fitted to the values of the blocks and enclosed volume on the log-log plot. The slopes of these straight lines can be taken as an estimation of the exponents of the power-law relation in Equation (1). The optimum threshold for separating geochemical anomalies from the

background is the concentration value common to both linear relationships on the Ln–Ln plot. The Ln–Ln plot of all the elements is shown in Fig. 4. As shown in these plots, for most elements, two levels of the threshold have been obtained. To select one of these two thresholds, the classical method also calculated the threshold, and each of the threshold obtained from the fractal method that is closest to the threshold of the classical method is selected as the final threshold. The thresholds specified by these plots are shown in Table 3. These thresholds are used in the zonality index method

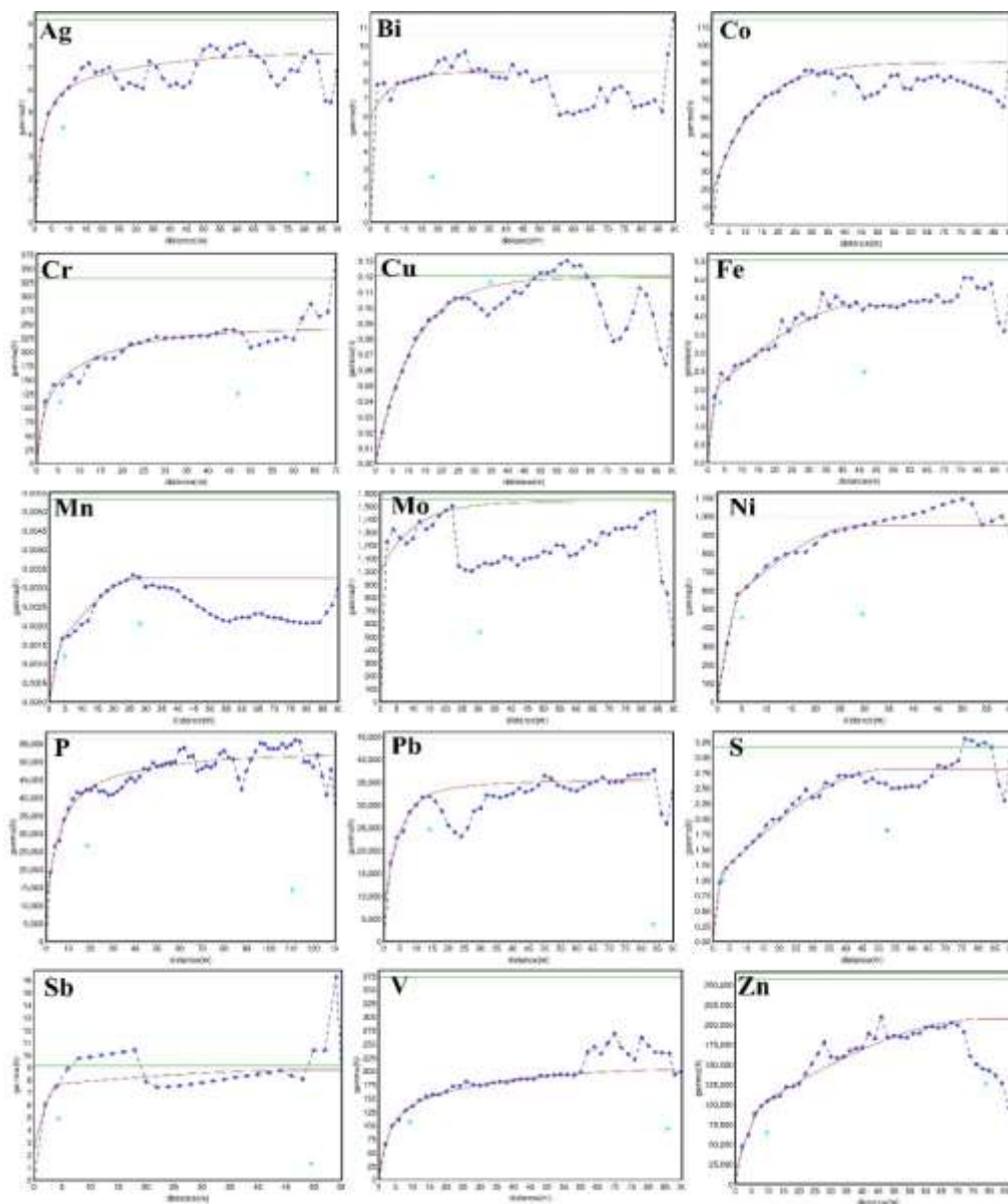


Fig. 3.- Major experimental variogram and fitted variogram models of Ag, Bi, Co, Cr, Cu, Fe, Mn, Mo, Ni, P, Pb, S, Sb, V, and Zn concentration data in Aliabad deposit

Table 2-. Anisotropy factors of the analyzed elements at the Aliabad deposit. Bi and Ni are showing week anisotropy, while S and Cu are showing strong anisotropy.

Elements	Major/Semimajor	Major/Minor
Ag	1.2	1.35
Bi	1.0	1.15
Co	1.45	1.6
Cr	1.0	1.4
Cu	1.65	2.1
Fe	1.2	1.45
Mn	1.15	1.55
Mo	1.7	1.95
Ni	1.0	1.2
P	1.4	1.4
Pb	1.35	1.4
S	1.9	2.25
Sb	1.1	1.25
V	1.2	1.35
Zn	1.25	1.6

Table 3-. Elemental thresholds identified using the C-V model and Classic Method ($\bar{X}+2S$). Bold and underlined values are selected thresholds based on each other that is more near to the classic threshold

Elements	First threshold	Second threshold	$\bar{X}+2S$
Ag (ppm)	2.34	6.36	3.85
Bi (ppm)	1.22	5.21	2.13
Co (ppm)	8.17	19.11	19.10
Cr (ppm)	11.94	37.34	30.08
Cu (%)	0.39	1.05	0.60
Fe (%)	3.00	3.00	5.21
Mn (%)	0.05	0.35	0.13
Mo (ppm)	24.53	70.11	44.95
Ni (ppm)	13.46	49.40	43.04
P (ppm)	314.19	632.70	709.03
Pb (ppm)	37.34	523.22	297.67
S (%)	1.28	3.56	3.88
Sb (ppm)	0.11	0.21	1.07
V (ppm)	13.46	54.60	41.05
Zn (ppm)	104.58	897.85	739.74

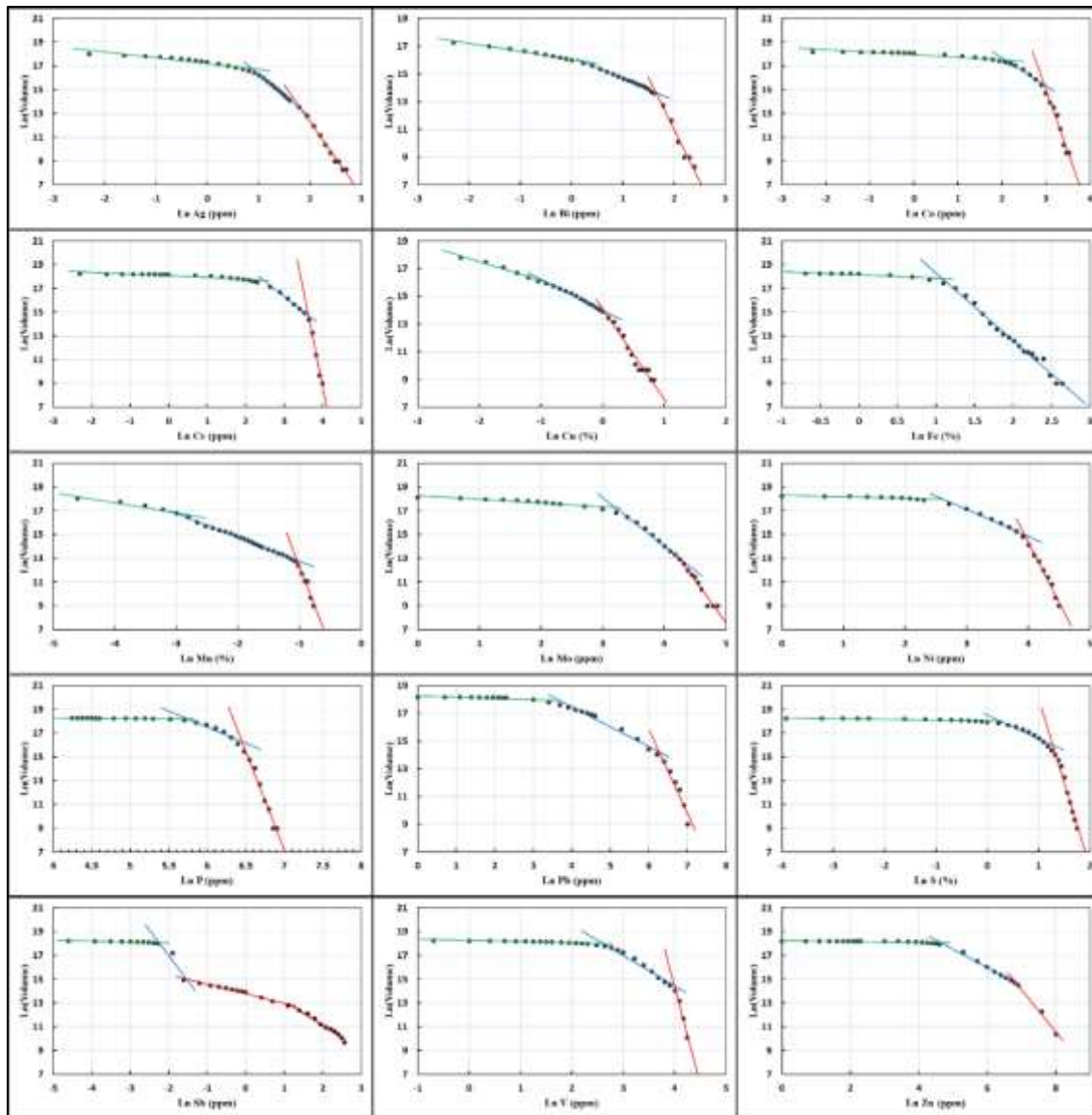


Fig. 4-. C-V Ln-Ln plots for Ag, Bi, Co, Cr, Cu, Fe, Mn, Mo, Ni, P, Pb, S, Sb, V and Zn

7- CONCEPT OF GEOCHEMICAL ZONALITY METHOD

In geochemical exploration, the determination of the erosion level of a geochemical anomaly relative to the depth of potential mineralization is very important as it helps to identify hidden minerals [28]. Kitaev (1991) proposed a multidimensional geochemical field analysis based on the notion that geological space is composed of geochemical fields representing the zonality of associations of chemical elements. This analysis takes into account the dispersion of chemical elements to separate multielement anomalies according to the values of Vz [29]. Grigorian (1992) has shown that patterns of geochemical zonality (Vz) around exposed deposits are distinct from patterns of Vz associated with blind deposits [30].

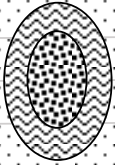
Recognition of zonality of geochemical halos associated with blind deposits can be achieved via four cases of complementary analyses [31]: (1) analysis of element associations representing supra-ore and sub-ore halos of mineral deposits; (2) analysis of a single component, implying false anomaly; (3) analysis of mean values of indicator elements outside significant geochemical anomalies to eliminate background noise in data analysis; and (4) mapping of multiplicative geochemical anomalies (i.e., Vz indices).

Figure 5 shows vertical variations in three Vz indices ($Vz_1 = Zn * Pb / Cu * Ag$, $Vz_2 = Pb * Zn / Cu * Mo$, $Vz_3 = Zn * Pb * Bi / Cu * Mo * Ag$) associated with porphyry-Cu deposits in areas of the same landscape-geochemical conditions in different countries. Values of each Vz index decrease downward uniformly despite considerable

differences in local geological settings of individual porphyry-Cu deposits, suggesting the existence of uniform vertical Vz in primary halos of porphyry-Cu deposits [30,32]. Therefore, vertical variations in values of Vz indices allow distinction of levels of mineralization and their primary (supra-ore, upper-ore, ore, lower-ore, and sub-ore) halos [30,33-34] (Fig. 5). Moreover, it can be deduced from Fig. 5 that similar values of a Vz index imply similar depths of mineralization and primary halos within an orefield. Thus, primary halos of mineral deposits at different depths are characterized by specific values of a Vz index the practical exploration significance of a Vz index is for recognition of erosional surfaces representing vertical levels of geochemical anomalies. That is because, in a Vz index, element data products used as numerators represent supra-ore to ore element associations whereas those used as denominators represent ore to sub-ore element

associations. With respect to the present level of erosion, high values of a Vz index imply the presence of sub cropping to blind deposits whereas low values of the index imply outcropping or already eroded deposits. Among the Vz indices shown in Fig. 5, the Vz₁, (or Zn*Pb/Cu*Ag) is the best indicator of blind porphyry-Cu deposits in general (i.e., those not enriched in a secondary metal such as Mo or Au) [32,35].

Although the Vz method was developed originally for analysis of litho-geochemical data [29], Grigorian (1992) has demonstrated that it can be applied to stream sediment geochemical data to analyze erosional surfaces of multiplicative anomalies representing different exhumation levels of mineral deposits [30]. Successful recognition of anomalous erosional surfaces is related, therefore, to the landscape conditions in mineralized regions [31].

Erosional surface	Vertical Section		$Vz_1 = \frac{Zn * Pb}{Cu * Ag}$	$Vz_2 = \frac{Zn * Pb}{Cu * Mo}$	$Vz_3 = \frac{Zn * Pb * Bi}{Cu * Mo * Ag}$
Supra-ore	I		>100	>5	>1
Upper ore	II		100 - 10	5 - 0.5	1 - 0.1
ore	III		10 - 1	0.5 - 0.05	0.1 - 0.01
ore	IV		1 - 0.1	0.05 - 0.005	0.01 - 0.001
Lower ore	V		0.1 - 0.01	0.005 - 0.0005	0.001 - 0.0001
sub-ore	VI		<0.01	<0.0005	<0.0001
		Contrast Vz(I)/Vz(VI)	10,000	10,000	10,000

 orebody
  enclosing rocks
  primary halo
  ground surface

Fig. 5-. Vertical geochemical zonality (Vz) models for porphyry-Cu deposits based on typical standard porphyry-Cu deposits in Kazakhstan, Bulgaria, Armenia, and Iran (from [35])

8- REGIONAL DISTRIBUTION OF ELEMENTS AND GEOCHEMICAL ZONALITY INDEX IN THE STUDY AREA

Zonality index is defined as the ratio of surface production power of each element at each level to the sum of the surface production power of the element at all levels. In this study, the zonality index for every analyzed element is calculated. For all the elements, the three-dimensional block model and then the map at different levels have been prepared. Here, the only block models and maps at two elevations of 2290 and 2430 m, corresponding to the Cu and Pb elements, are shown in Fig. 6 and Fig. 7. As shown in the block model and the maps, the amount of copper increases with greater depths. According to the block model and maps of Pb at

different levels, the amount of Pb in the surface is high and decreases in depth.

Since the vertical zoning of the primary haloes is a criterion for determining the level of erosion of the geochemical anomalies relative to the ore deposit, the sequence of elemental depth-to-depth zoning is investigated first. To obtain the vertical zonality of the primary haloes, the surface production power of the elements at each level (The product of a surface area greater than a threshold obtained by the C-V fractal method at the mean value larger than that threshold) was used (Table 3). Table 3 shows the highest surface zonality for each element in the elevation column, as well as Fig. 8 graphically represents the zonality index at different depths for each element. As the result, the following sequence can be considered for elements from the surface to the bottom: Pb → (Bi, Mn, Mo) → Cr → Ni → (Sb, V, Zn) → (Ag, Co, Cu, Fe, S) → P.

Since the studied deposit is a porphyry copper deposit, Vertical geochemical zonality (Vz) models for porphyry–Cu deposits based on typical standard porphyry–Cu deposits have been used ($Vz_1=Zn*Pb/Cu*Ag$, $Vz_2=Pb*Zn/Cu*Mo$, $Vz_3=Zn*Pb*Bi/Cu*Mo*Ag$). In addition, according to the zoning index diagrams Fig. 8 and Table 3, two geochemical zonality indices are exclusively introduced for the study area ($Vz_4=Pb*Mn/Cu*Ag$ and $Vz_5=Pb*Mn/Cu*Ag*Co$).

By plotting erosion surface maps derived from the multiplication of haloes ratio, areas with higher and lower levels of mineralization were identified. According to Fig. 5 which is a vertical geochemical zonality model (Vz) for typical porphyry copper deposits ($Vz_1=Zn*Pb/Cu*Ag$, $Vz_2=Pb*Zn/Cu*Mo$, $Vz_3=Zn*Pb*Bi/Cu*Mo*Ag$) and obtained according to the zonality of different elements in this

study ($Vz_4=Pb*Mn/Cu*Ag$ and $Vz_5=Pb*Mn/Cu*Ag*Co$).

Considering the block model and horizontal sections of the block model at 2290 and 2430 m elevations (Fig. 9), it can be concluded that mineralization does exist at the northwestern and also southern parts of the area.

In the northwest of the study area, the deposit is at the Supra-Ore level, indicating that there is no outcrop in this area and implying a hidden deep deposit. Therefore, it is highly recommended to drill additional boreholes in these areas. It is noteworthy that new drillings of the northwestern part must continue deeper than current boreholes (>150 m); because geochemical zonality indexes are expanded to deeper parts. This expansion is not observed for the southern parts, so, there is no need for additional drillings at the southern part to go deeper than 150 m.

Table 4-. Zonality index of elements at different levels in the study area

Zonality Index								
Level	Ag	Bi	Co	Cr	Cu	Fe	Mn	Mo
2440	0.061	0.098	0.039	0.061	0.000	0.040	0.119	0.102
2420	0.064	0.107	0.048	0.129	0.013	0.059	0.130	0.123
2400	0.064	0.111	0.071	0.168	0.016	0.091	0.132	0.133
2380	0.077	0.101	0.114	0.186	0.031	0.121	0.128	0.132
2360	0.103	0.106	0.151	0.171	0.100	0.143	0.122	0.126
2340	0.130	0.111	0.181	0.145	0.165	0.151	0.112	0.121
2320	0.149	0.106	0.192	0.105	0.208	0.147	0.094	0.108
2300	0.146	0.108	0.129	0.036	0.206	0.126	0.076	0.094
2280	0.129	0.097	0.076	0.000	0.174	0.087	0.055	0.054
2260	0.078	0.056	0.000	0.000	0.088	0.034	0.032	0.006
Zonality Index								
Level	Ni	P	Pb	S	Sb	V	Zn	Element with maximum zonality Index
2440	0.044	0.000	0.180	0.000	0.017	0.077	0.039	Pb
2420	0.112	0.019	0.165	0.000	0.023	0.099	0.036	
2400	0.149	0.033	0.138	0.027	0.073	0.117	0.013	(Bi, Mn, Mo)
2380	0.161	0.054	0.114	0.075	0.193	0.131	0.087	Cr
2360	0.170	0.090	0.097	0.121	0.233	0.138	0.163	Ni
2340	0.162	0.139	0.086	0.166	0.229	0.135	0.192	(Sb, V, Zn)
2320	0.125	0.178	0.074	0.203	0.157	0.123	0.180	(Ag, Co, Cu, Fe, S)
2300	0.059	0.192	0.064	0.197	0.071	0.099	0.142	P
2280	0.018	0.183	0.051	0.155	0.004	0.061	0.100	
2260	0.000	0.112	0.030	0.055	0.000	0.020	0.048	

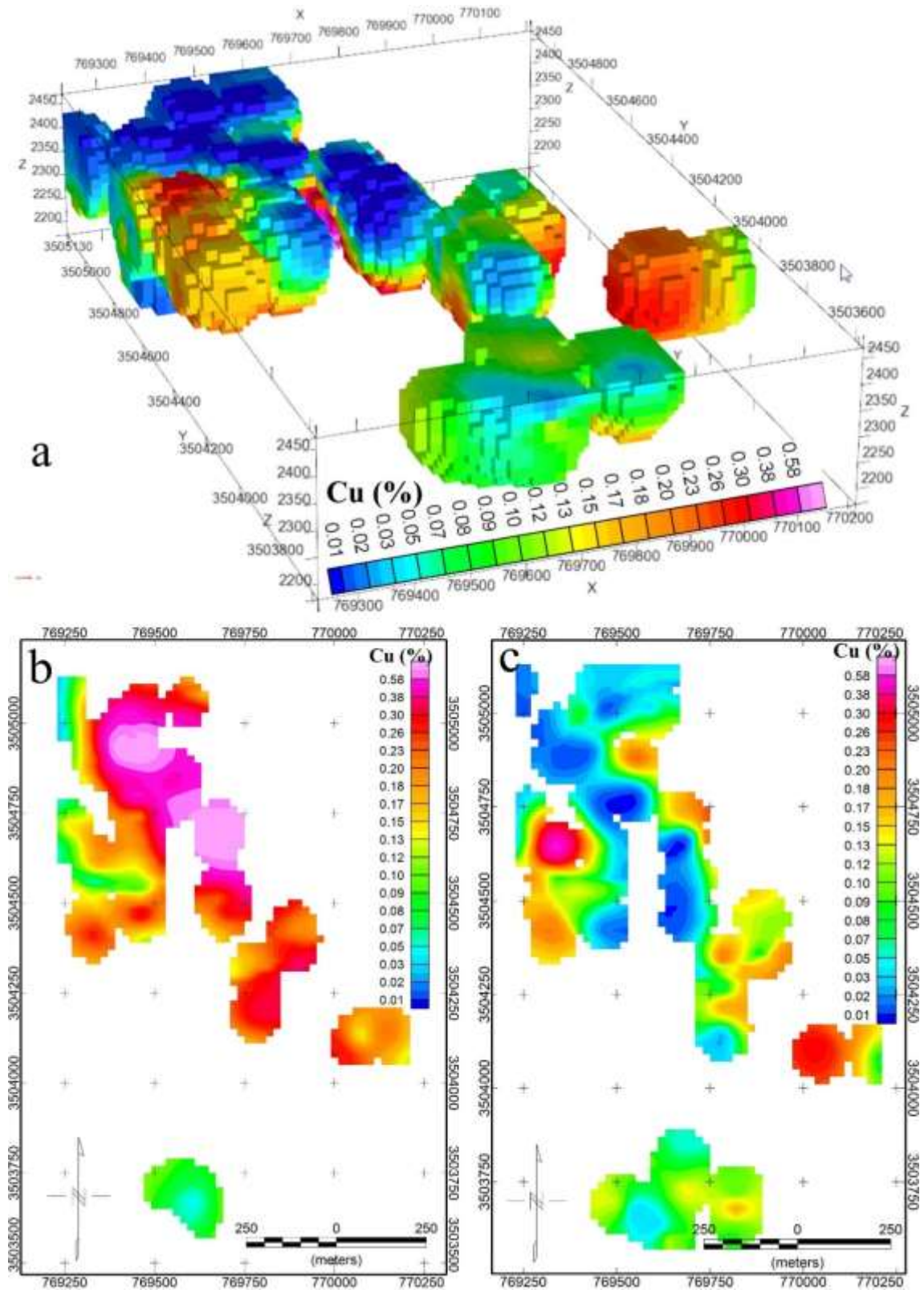


Fig. 6-. a. Cu concentration block model and horizontal section maps of the block model at b. 2290 and c. 2430 meters elevations

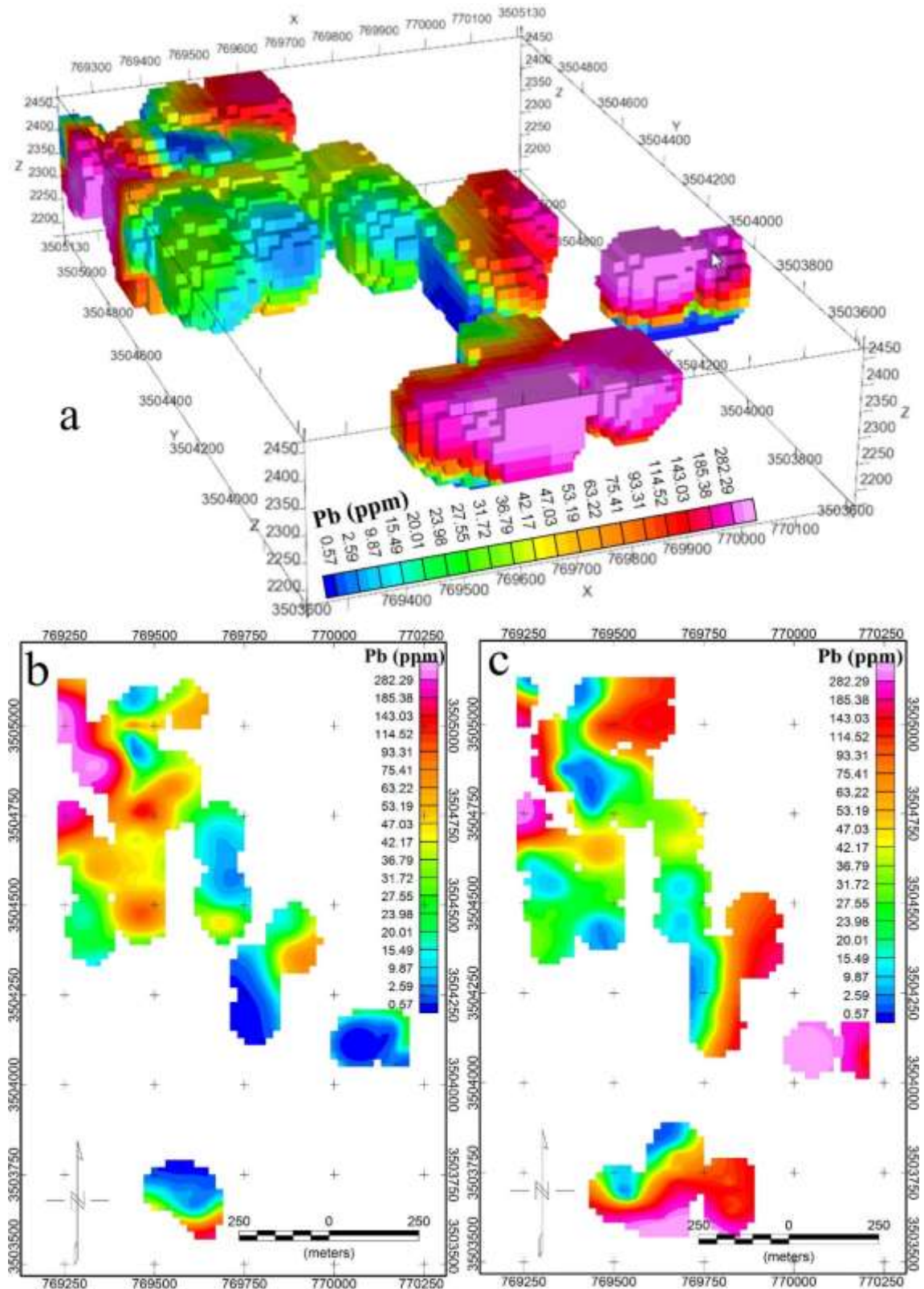


Fig. 7-. a. Pb concentration block model and horizontal section maps of the block model at b. 2290 and c. 2430 meters elevations

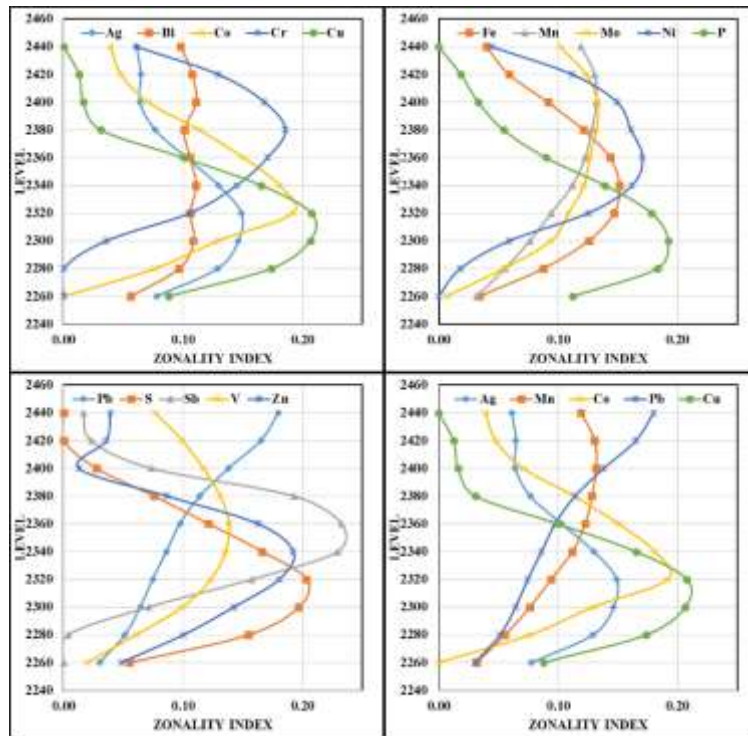


Fig. 8-. Zonality index of elements at different levels and selected upper ore and lower ore elements (Ag, Mn, Co, Pb, Cu) in the study area (bottom right)

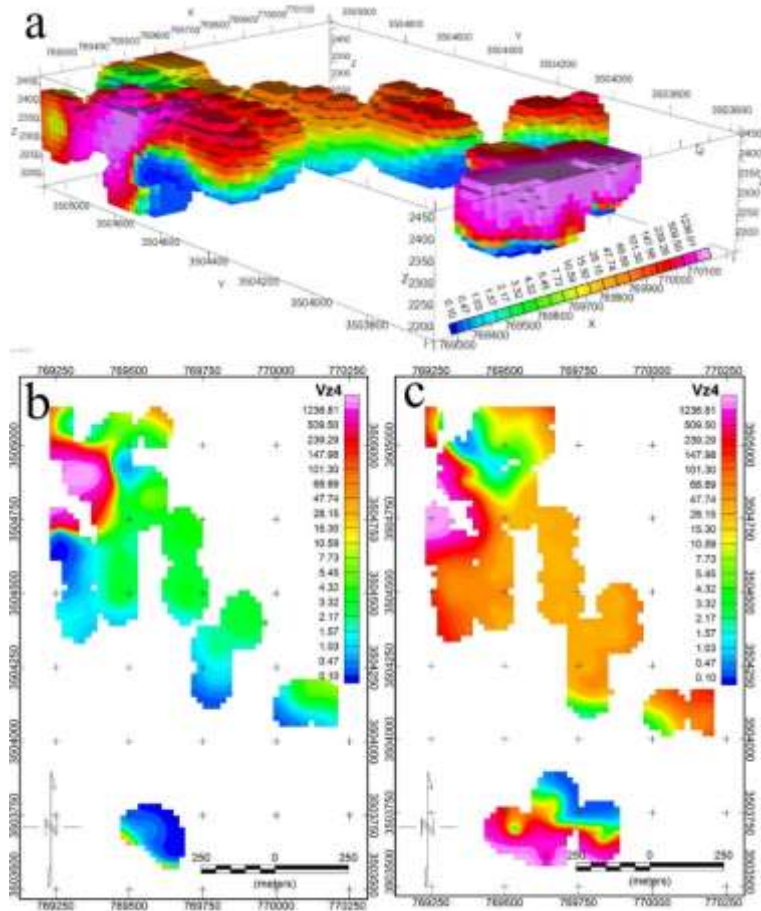


Fig. 9-. a. Vz_4 concentration block model and horizontal section maps of the block model at b. 2290 and c. 2430 meters elevations

9- CONCLUSIONS

In this study, the Aliabad copper deposit was studied to determine erosion level and to investigate possible deeper mineralization by determination of zonality index. This study was carried out using elemental distribution as well as zoning sequences at different levels and also, appropriate zonality index. The results can be presented as follow:

1. Based on the modeled zonality index, the sequence of upper ore to lower ore elements of the study area can be determined as follow: Pb → (Bi, Mn, Mo) → Cr → Ni → (Sb, V, Zn) → (Ag, Co, Cu, Fe, S) → P.
2. Regarding this zoning, two zonality indexes ($V_{Z4} = \text{Pb} * \text{Zn} / \text{Cu} * \text{Fe}$, $V_{Z5} = \text{Pb} * \text{Zn} * \text{Ca} / \text{Cu} * \text{Fe} * \text{Co}$) were introduced. Among these two indexes, V_{Z4} is considered to be more appropriate.
3. According to the V_z index at the block model and zonality index distribution maps, it can be concluded that mineralization does exist at the northwestern and also southern parts of the area. In the northwest of the study area, the deposit is at the Supra-Ore level, indicating that there is no outcrop in this area and implying a hidden deep deposit and in the south of the study area, the deposit is at the upper ore level.
4. Therefore, additional drillings are highly recommended in these areas. Because geochemical zonality indexes are expanded to deeper parts at the northwestern part, new drillings must continue deeper than the current boreholes (>150 m). This extension is not observed for the southern parts, so, additional drillings at the southern part do not need to go deeper than 150 m.

REFERENCES

- [1] Safronov, N. I. (1936) Dispersion haloes of ore deposits and their use in exploration. *Probl. Sov. Geol.* 4, 41–53.
- [2] Li, Y., Zhang, D., Dai, L., Wan, G. and Hou, B. (2016) Characteristics of structurally superimposed geochemical haloes at the polymetallic Xiasai silver-lead-zinc ore deposit in Sichuan Province, SW China. *J. Geochemical Explor., Elsevier B.V.* 169, 100–122.
- [3] Carranza, E. J. M. (2012) Primary geochemical characteristics of mineral deposits: implications for exploration. *Ore Geol. Rev., Elsevier* 45, 1–4.
- [4] Goldberg, I. S., Abramson, G. Y. and Los, V. L. (2003) Depletion and enrichment of primary haloes: their importance in the genesis of and exploration for mineral deposits. *Geochemistry Explor. Environ. Anal., Geological Society of London* 3, 281–293.
- [5] Govett, G. J. S. 1983, *Rock geochemistry in mineral exploration: Handbook of exploration geochemistry*, v. 3, Amsterdam, Elsevier.
- [6] Bierlein, F. P., Fuller, T., Stüwe, K., Arne, D. C. and Keays, R. R. (1998) Wallrock alteration associated with turbidite-hosted gold deposits. Examples from the Palaeozoic Lachlan Fold Belt in central Victoria, Australia. *Ore Geol. Rev., Elsevier* 13, 345–380.
- [7] Hannington, M. D., Santaguida, F., Kjarsgaard, I. M. and Cathles, L. M. (2003) Regional-scale hydrothermal alteration in the Central Blake River Group, western Abitibi subprovince, Canada: implications for VMS prospectivity. *Miner. Depos., Springer* 38, 393–422.
- [8] Beus, A. A. and Grigorian, S. V. (1977) *Geochemical exploration methods for mineral deposits*, Applied Publishing Ltd., Wilmette, IL.
- [9] Xie, X. and Shao, Y. (1965) The method of work and interpretation of geochemical rock survey. *Geophys. Geochem. Explor. Res. Bull.* 5, 2–7.
- [10] Chongmin, L. and Waisheng, X. (1995) Primary geochemical anomalies in the Caijiaying Pb-Zn-Ag deposits, Hebei, China. *J. Geochemical Explor.* 55, 25–32.
- [11] Liu, C., Hu, S., Ma, S. and Tang, L. (2014) Primary geochemical patterns of Donggua Mountain laminar skarn copper deposit in Anhui, China. *J. Geochemical Explor., Elsevier B.V.* 139, 152–159.
- [12] Harris, J. R., Wilkinson, L. and Grunsky, E. C. (2000) Effective use and interpretation of lithochemical data in regional mineral exploration programs: application of Geographic Information Systems (GIS) technology. *Ore Geol. Rev., Elsevier* 16, 107–143.
- [13] Ziaii, M., Carranza, E. J. M. and Ziaei, M. (2011) Application of geochemical zonality coefficients in mineral prospectivity mapping. *Comput. Geosci., Elsevier* 37, 1935–1945.
- [14] Berberian, M. and King, G. C. P. (1981) Towards a paleogeography and tectonic evolution of Iran. *Can. J. Earth Sci., NRC Research Press* 18, 210–265.
- [15] Amooyi Ardakani, A. (1998) Investigation of Petrology of Kheyr Abad Intrusive Mass, Shahid Beheshti University.
- [16] Padir Consulting Engineers. (2001) *Geological Surveys of Ali Abade Yazd.*
- [17] John, D. A., Ayuso, R. A., Barton, M. D., Bodnar, R. J., Dilles, J. H., Gray, F., Graybeal, F. T., Mars, J. C., McPhee, D. K., Seal, R. R., et al. (2010) *Porphyry Copper Deposit Model Scientific Investigations Report 2010 – 5070 – B. USGS Sci. Investig. Rep. 2010-5070-B* 169.
- [18] Lowell, J. D. and Guilbert, J. M. (1970) Lateral and vertical alteration-mineralization zoning in porphyry ore deposits. *Econ. Geol., Society of Economic Geologists* 65, 373–408.
- [19] Bemani, M., Mojtahedzade, S. H. and Ansari, A. (2020) Geology, petrology, alteration and mineralization of Aliabad-Damak copper ore deposit. *Iran. J. Crystallogr. Mineral. under revi.*
- [20] Samiee, S., Karimpoor, M. H., Ghaderi, M. and Heydarian Shahri, M. R. (2013) Geology, alteration, mineralization and geochemistry of Khunik area, south of Birjand. *Iran. J. Crystallogr. Mineral.* 21, 487–498.
- [21] Miri Beydokhti, R., Karimpour, M. H. and Mazaheri, S. A. (2014) Studies of remote sensing, geology, alteration, mineralization and geochemistry of

Balazard copper-gold prospecting area, west of Nehbandan. Iran. J. Crystallogr. Mineral. 22, 459–470.

[22] Azadi, M., Mirmohammadi, M. and Hezarkhani, A. (2014) Petrology and fluid inclusion studies in Kahang porphyry copper deposit. Iran. J. Crystallogr. Mineral. 22, 155–172.

[23] Kaviani, A., Hatzfeld, D., Paul, A., Tatar, M. and Priestley, K. (2009) Shear-wave splitting, lithospheric anisotropy, and mantle deformation beneath the Arabia-Eurasia collision zone in Iran. Earth Planet. Sci. Lett. 286, 371–378.

[24] Molayemat, H., Torab, F. M., Pawlowsky-Glahn, V., Hossein Morshedy, A. and Egozcue, J. J. (2018) The impact of the compositional nature of data on coal reserve evaluation, a case study in Parvadeh IV coal deposit, Central Iran. Int. J. Coal Geol., Elsevier 188, 94–111.

[25] Afzal, P., Alghalandis, Y. F., Khakzad, A., Moarefvand, P. and Omran, N. R. (2011) Delineation of mineralization zones in porphyry Cu deposits by fractal concentration--volume modeling. J. Geochemical Explor., Elsevier 108, 220–232.

[26] Afzal, P., Dadashzadeh, H., Rashidnejad, N. and Aliyari, F. (2013) Delineation of gold mineralized zones using concentration – volume fractal model in Qolqoleh gold deposit, NW Iran. Ore Geol. Rev., Elsevier B.V. 55, 125–133.

[27] Afzal, P., Hosein, S., Tokhmechi, B. and Kaveh, D. (2014) International Journal of Coal Geology Outlining of high quality coking coal by concentration – volume fractal model and turning bands simulation in East-Parvadeh coal deposit, Central Iran. Int. J. Coal Geol., Elsevier B.V. 127, 88–99.

[28] Hassani Pak, A. A. (2010) Principles of geochemical exploration, University of Tehran Press. Tehran.

[29] Kitaev, N. A. (1991) Multidimensional analysis of geochemical fields. Math. Geol., Springer 23, 15–32.

[30] Grigorian, S. V. (1992) Mining geochemistry. Nedra, Moscow.

[31] Ziaii, M., Pouyan, A. A. and Ziaei, M. (2009) Neuro-fuzzy modelling in mining geochemistry: identification of geochemical anomalies. J. Geochemical Explor., Elsevier 100, 25–36.

[32] Ziaii, M., Abedi, A. and Ziaei, M. (2009) Geochemical and mineralogical pattern recognition and modeling with a Bayesian approach to hydrothermal gold deposits. Appl. Geochemistry, Elsevier 24, 1142–1146.

[33] Solovov, A. P. and Kuznetov, V. V. (1987) Geochemical prospecting for mineral deposits, Mir Publ.

[34] Solovov, A. P. (1990) Handbook on geochemical prospecting for useful minerals, Nedra Publishing House, Moscow [in Russian].

[35] Ziaii, M. (1996) Litho-geochemical exploration methods for copper-porphyry deposit in Sungun, NW Iran. Unpubl. M. Sc. thesis. Geochemistry Fac. MSU, Moscow.